



HAL
open science

Relevance of Brain Regions Eloquence Assessment in Patients with Large Ischemic Cores treated with Mechanical Thrombectomy

Basile Kerleroux, Joseph Benzakoun, Kévin Janot, Cyril Dargazanli, Dimitri Daly Eraya, Wagih Ben Hassen, François Zhu, Benjamin Gory, Hak Jean-Francois, Charline Perot, et al.

► To cite this version:

Basile Kerleroux, Joseph Benzakoun, Kévin Janot, Cyril Dargazanli, Dimitri Daly Eraya, et al.. Relevance of Brain Regions Eloquence Assessment in Patients with Large Ischemic Cores treated with Mechanical Thrombectomy. *Neurology*, 2021, 97 (20), pp.e1975-e1985. 10.1212/WNL.0000000000012863 . inserm-03403995

HAL Id: inserm-03403995

<https://inserm.hal.science/inserm-03403995>

Submitted on 26 Oct 2021

HAL is a multi-disciplinary open access archive for the deposit and dissemination of scientific research documents, whether they are published or not. The documents may come from teaching and research institutions in France or abroad, or from public or private research centers.

L'archive ouverte pluridisciplinaire **HAL**, est destinée au dépôt et à la diffusion de documents scientifiques de niveau recherche, publiés ou non, émanant des établissements d'enseignement et de recherche français ou étrangers, des laboratoires publics ou privés.

Relevance of Brain Regions Eloquence Assessment in Patients with Large Ischemic Cores treated with Mechanical Thrombectomy.

Author(s):

Basile Kerleroux, MD; Joseph Benzakoun, MD; Kévin Janot, MD; Cyril Dargazanli, MD; Dimitri Daly Eraya, MD; Wagih Ben Hassen, MD; François Zhu, MD; Benjamin Gory, MD-PhD; Jean-Francois HAK, MD; Charline Perot, MD; Lili Detraz, MD; Romain Bourcier, MD-PhD; Rouchaud Aymeric, MD-PhD; Géraud Forestier, MD; Gaultier Marnat, MD; Florent Gariel, MD; Pasquale Mordasini, MD; Pierre Seners, MD-PhD; Guillaume Turc, MD-PhD; Johannes Kaesmacher, MD; Catherine Oppenheim, MD; Olivier Naggara, MD-PhD; Gregoire Boulouis, MD on behalf of the JENI Research Collaborative

Equal Author Contributions:

Basile Kerleroux and Joseph Benzakoun contributed equally to this work; Special designations : "co-first authors"

Corresponding Author:

Basile Kerleroux

basile.kerleroux@gmail.com

Affiliation Information for All Authors: Basile KERLEROUX, INSERM U1266, Institut of Psychiatry and Neuroscience (IPNP), UMR_S1266, INSERM, Université de Paris, GHU Paris Psychiatrie et Neurosciences, site Sainte-Anne, Joseph BENZAKOUN, INSERM U1266, Institut of Psychiatry and Neuroscience (IPNP), UMR_S1266, INSERM, Université de Paris, GHU Paris Psychiatrie et Neurosciences, site Sainte-Anne, Kevin JANOT, Diagnostic and Therapeutic Neuroradiology, CHRU de Tours, 2 bd Tonnelé, Tours France Cyril DARGAZANLI, Department of Interventional Neuroradiology, University Hospital Center of Montpellier, Gui de Chauliac hospital, Montpellier, France Dimitri DALY ERAYA, Department of Interventional Neuroradiology, University Hospital Center of Montpellier, Gui de Chauliac hospital, Montpellier, France Wagih BEN HASSEN, INSERM U1266, Institut of Psychiatry and Neuroscience (IPNP), UMR_S1266, INSERM, Université de Paris, GHU Paris Psychiatrie et Neurosciences, site Sainte-Anne, François ZHU, Université de Lorraine, CHRU-Nancy, Department of Diagnostic and Therapeutic Neuroradiology, F-54000 Nancy, France and Université de Lorraine, IADI, INSERM U1254, F-54000 Nancy, France Benjamin GORY, Université de Lorraine, CHRU-Nancy, Department of Diagnostic and Therapeutic Neuroradiology, F-54000 Nancy, France and Université de Lorraine, IADI, INSERM U1254, F-54000 Nancy, France Jean François HAK, Department of Diagnostic and Interventional Neuroradiology, Timone Hospital, Aix Marseille University, APHM, Cedex, France Charline PEROT, Neurology Department, Timone Hospital, Aix Marseille University, APHM, Cedex, France. Lili DETRAZ, Department of Diagnostic and Interventional Neuroradiology, Guillaume et René Laennec University Hospital, Nantes, France Romain BOURCIER, Department of Diagnostic and Interventional Neuroradiology, Guillaume et René Laennec University Hospital, Nantes, France Aymeric ROUCHAUD, Department of interventional neuroradiology, Dupuytren University Hospital, 2 Avenue Martin Luther King, 87000 Limoges, France. Géraud FORESTIER, Department of interventional neuroradiology, Dupuytren University Hospital, 2 Avenue Martin Luther King, 87000 Limoges, France. Gaultier MARNAT, Department of Diagnostic and Interventional Neuroradiology, Pellegrin Hospital - University Hospital of Bordeaux, Place Amélie Raba-Léon, 33076 Bordeaux, France. Florent GARIEL, Department of Diagnostic and Interventional Neuroradiology, Pellegrin Hospital - University Hospital of Bordeaux, Place Amélie Raba-Léon, 33076 Bordeaux, France. Pasquale MORDASINI, Institute of Diagnostic, Interventional and Pediatric Radiology and Institute of Diagnostic and Interventional Neuroradiology, University Hospital Bern, Inselspital, University of Bern, Bern, Switzerland Pierre SENERS, Neurology Department, Fondation Rothschild Hospital, Paris, France Guillaume TURC, Neurology Department, GHU Paris Psychiatrie et Neurosciences,

Université de Paris, INSERM U1266, FHU NeuroVasc, Paris, France Johannes KAESMACHER, Institute of Diagnostic, Interventional and Pediatric Radiology and Institute of Diagnostic and Interventional Neuroradiology, University Hospital Bern, Inselspital, University of Bern, Bern, Switzerland Catherine OPPENHEIM, INSERM U1266, Institut of Psychiatry and Neuroscience (IPNP), UMR_S1266, INSERM, Université de Paris, GHU Paris Psychiatrie et Neurosciences, site Sainte-Anne, Olivier NAGGARA, INSERM U1266, Institut of Psychiatry and Neuroscience (IPNP), UMR_S1266, INSERM, Université de Paris, GHU Paris Psychiatrie et Neurosciences, site Sainte-Anne, Grégoire BOULOUIS, Neuroradiology Department, Université de Paris, des Neurosciences Psychiatrie de Paris, Diagnostic and Therapeutic Neuroradiology, CHRU de Tours, 2 bd Tonnelé, Tours France

Contributions:

Basile Kerleroux: Drafting/revision of the manuscript for content, including medical writing for content; Major role in the acquisition of data; Study concept or design; Analysis or interpretation of data

Joseph Benzakoun: Drafting/revision of the manuscript for content, including medical writing for content; Major role in the acquisition of data; Study concept or design; Analysis or interpretation of data

Kévin Janot: Drafting/revision of the manuscript for content, including medical writing for content; Major role in the acquisition of data

Cyril Dargazanli: Major role in the acquisition of data

Dimitri Daly Eraya: Major role in the acquisition of data

Wagih Ben Hassen: Major role in the acquisition of data

François Zhu: Major role in the acquisition of data

Benjamin Gory: Drafting/revision of the manuscript for content, including medical writing for content; Major role in the acquisition of data

Jean-Francois HAK: Drafting/revision of the manuscript for content, including medical writing for content; Major role in the acquisition of data

Charline Perot: Major role in the acquisition of data

Lili Detraz: Major role in the acquisition of data

Romain Bourcier: Major role in the acquisition of data

Rouchaud Aymeric: Drafting/revision of the manuscript for content, including medical writing for content; Major role in the acquisition of data

Géraud Forestier: Major role in the acquisition of data

Gaultier Marnat: Drafting/revision of the manuscript for content, including medical writing for content; Major role in the acquisition of data

Florent Gariel: Major role in the acquisition of data

Pasquale Mordasini: Drafting/revision of the manuscript for content, including medical writing for content

Pierre Seners: Drafting/revision of the manuscript for content, including medical writing for content; Major role in the acquisition of data

Guillaume Turc: Drafting/revision of the manuscript for content, including medical writing for content

Johannes Kaesmacher: Drafting/revision of the manuscript for content, including medical writing for content; Major role in the acquisition of data; Study concept or design

Catherine Oppenheim: Drafting/revision of the manuscript for content, including medical writing for content

Olivier Naggara: Drafting/revision of the manuscript for content, including medical writing for content; Study concept or design; Analysis or interpretation of data

Gregoire Boulouis: Drafting/revision of the manuscript for content, including medical writing for content; Major role in the acquisition of data; Study concept or design; Analysis or interpretation of data

Number of characters in title: 94

Abstract Word count: 254

Word count of main text: 3994

References: 31

Figures: 3

Tables: 2

Supplemental: STROBE Checklist; Collaborators Lists (X2)

Statistical Analysis performed by: Dr B. Kerleroux - MD-MCs, Neuroradiology-department, GHU-Paris, 1 rue Cabanis, 75014 Paris. basile.kerleroux@gmail.com Tel: +33145658574 Fax: +33145658574

Search Terms: [6] Infarction

The authors report no targeted funding

Disclosures: Dr Basile KERLEROUX reports no disclosures. Dr Joseph BENZAKOUN reports no disclosures. Dr Kevin JANOT reports no disclosures. Dr Cyril DARGAZANLI reports no disclosures. Dr Dimitri DALY ERAYA reports no disclosures. Dr Wagih BEN HASSEN reports no disclosures. Dr François ZHU reports no disclosures. Dr Benjamin GORY reports no disclosures. Dr Jean François HAK reports no disclosures. Dr Charline PEROT reports no disclosures. Dr Lili DETRAZ reports no disclosures. Dr Romain BOURCIER reports no disclosures. Dr Aymeric ROUCHAUD reports no disclosures. Dr Géraud FORESTIER reports no disclosures. Dr Gaultier MARNAT reports no disclosures. Dr Florent GARIEL reports no disclosures. Dr Pasquale MORDASINI reports no disclosures. Dr Pierre SENERS reports no disclosures. Dr Guillaume TURC reports no disclosures. Dr Johannes KAESMACHER reports no disclosures. Dr Catherine OPPENHEIM reports no disclosures. Dr Olivier NAGGARA reports no disclosures. Dr Grégoire BOULOUIS reports no disclosures.

ABSTRACT

Objective

Individualized patient selection for mechanical thrombectomy (MT) in patients with acute ischemic stroke (AIS) and large volume of severely ischemic tissue of uncertain viability (SIT-uv, or large ischemic core LIC) at baseline is an unmet need. We tested the hypothesis, that assessing the functional relevance of both the infarcted and hypo-perfused brain tissue, would improve the selection framework of patients with LIC for MT.

Methods

Multicenter, retrospective, study of adult with LIC (DWI volume \geq 70ml), with MRI perfusion, treated with MT or best medical management (BMM).

Primary outcome was 3-month modified-Rankin-Scale (mRS), favourable if 0-3. Global and regional-eloquence-based core-perfusion mismatch ratios were derived. The predictive accuracy for clinical outcome of eloquent regions involvement was compared in multivariable and bootstrap-random-forest models.

Results

A total of 138 patients with baseline LIC were included (MT n=96 or BMM n=42; mean age \pm SD, 72.4 \pm 14.4 years; 34.1% females; mRS=0-3: 45.1%). Mean core and critically-hypo-perfused volume were 100.4ml \pm 36.3ml and 157.6 \pm 56.2ml respectively and did not differ between groups. Models considering the functional relevance of the infarct location showed a better accuracy for the prediction of mRS=0-3 with a c-Statistic of 0.76 and 0.83 for logistic regression model and bootstrap-random-forest testing sets respectively. In these models, the interaction between treatment effect of MT and the mismatch was significant (p=0.04). In comparison in the logistic regression model disregarding functional eloquence the c-Statistic was 0.67 and the interaction between MT and the mismatch was insignificant.

Conclusion

Considering functional eloquence of hypo-perfused tissue in these patients allows for a more precise estimation of treatment expected benefit.

GLOSSARY

AIC = acute ischemic stroke; **LVO** = large vessel occlusion; **ASPECTS** = Alberta-Stroke-Program-Early-CT-score; **MT** = Mechanical Thrombectomy; **SIT-uv** = severely ischemic tissue of uncertain viability; **BMM** = best medical management; **mRS** = modified Rankin Scale; **i.v.tPA** = intravenous tissue plasminogen activator; **VLSM** = voxel-based lesion symptom mapping; **HE** = brain regions with high eloquence; **HE-I** = high-eloquence infarct; **HE-P** = high-eloquence critically hypo-perfused tissue; **E-MR** = eloquent mismatch ratios; **HE-MR** = high eloquence mismatch ratio; **G-I** = global infarct volume; **G-MR** = global mismatch ratio; **NNT** = number needed to treat;

INTRODUCTION

Patients with acute ischemic stroke (AIS) due to anterior large vessel occlusion (LVO) and an unfavourable imaging profile at baseline were excluded in 4 of the 7 randomized clinical trials that validated mechanical thrombectomy (MT),¹ precluding to draw strong conclusions regarding the benefits of MT in this subgroup.^{2,3}

A unfavourable imaging profile, is commonly defined as a large volume of severely ischemic tissue of uncertain viability (SIT-uv, or large ischemic core LIC), assessed using MRI diffusion weighted imaging volume (DWI, core > 70ml), or the CT-based-Alberta-Stroke-Program-Early-CT-score (ASPECTS < 6), and is amongst the most common reasons to decline MT in clinical practice due to potential futility.

Yet, evidence is growing that a subsample of patients with a LIC at baseline may benefit from revascularization, even if outside currently validated eligibility criteria for MT⁴, leading AHA and European recommendations to reconsider this subgroup as potentially eligible on a case by case evaluation of anticipated benefit.^{2,3}

Perfusion imaging can be used in the diagnostic work-up of AIS to identify hypo-perfused yet not infarcted (i.e. 'at-risk' or 'salvageable') brain tissue,⁵ and recent data have demonstrated its added value⁶ for the selection of patients with a deemed unfavourable imaging profile before MT, contributing to the accumulating evidence on the key role of tissue-based evaluation in patients with AIS-LVO.^{7,8}

Moving forward, the involvement of specific "eloquent" brain regions within the infarcted core has been shown to be of high relevance for determining functional outcome,⁹⁻¹² suggesting a greater benefit of revascularization for patients with salvageable eloquent regions. Identifying persistent salvageable eloquent brain areas is especially relevant in patients with large baseline infarct volumes to reduce over-selection (that is, to decline MT to a patient that may have benefited from revascularization). In that sense, considering the functional relevance of both

infarcted and hypo-perfused brain tissue in the framework of patients' selection may help improve individualized decision making.

In a large multicentric retrospective cohort of patients with an AIS due to large vessel occlusion and a large ischemic cores at presentation, we tested the hypothesis that the integration of the regional functional relevance of both infarcted and salvageable tissue would enhance the accurate detection of patients likeliest to benefit from endovascular revascularization.

METHODS

Study design & Ethics

Analyses used data from a multicenter, retrospective, core lab adjudicated, cohort study of patients with proximal vessel occlusion, a large ischemic core (initially set as a DWI-ASPECTS of 0-6 in order to simplify recruitment, but finally redefined after quantitative core measures as DWI core volume ≥ 70 cc), with pre-treatment MRI perfusion, treated with MT (2015-2018) or best medical management alone (BMM; before 2015). This cohort has been described in details elsewhere,⁶ and results from the collaborative work of a trainee-led research network (Jeunes en Neuroradiologie Interventionnelle, JENI).¹³ All the patients included in the current analysis have been previously reported in a distinct manuscript with a larger study sample.⁶ The prior report was focused on the overall core/perfusion mismatch influence on MT for AIS-LIC patients independent of brain eloquence, whereas in this manuscript, the analyses are aimed to determined the relevance of eloquent core/perfusion mismatch in determining anticipated treatment benefit.

This report was prepared according to the Strengthening the Reporting of Observational Studies in Epidemiology (STROBE) statement.¹⁴ As for all non-interventional retrospective studies of de-identified data, written informed consent was waived and a commitment to compliance (Reference Methodology CPMR-4)

was filed to the National Information Science and Liberties Commission prior to data centralization, in respect to the General Data Protection Regulation. Patients and proxies were informed they could oppose the use of their data for research purposes.

Inclusion and exclusion criteria

As developed elsewhere,⁶ we included consecutive adult patients with AIS, an occlusion of the intracranial internal carotid artery or of the M1 segment of the middle cerebral artery, a large pretreatment ischemic core volume defined as 70ml or more on MR-DWI as assessed centrally, no preexisting handicap (modified Ranking scale, mRs >1), and if pre-treatment DSC (dynamic susceptibility contrast) perfusion sequence had been performed. Patients were collected by retrospectively querying the prospective MT stroke data bases at eight university hospitals (MT group) and the prospective i.v. tPA stroke data base at a single university hospital (BMM group, not treated with MT). The control group included patients treated before MT-related guidelines in 2015 and was obtained from a single center at which perfusion imaging was routinely performed at the acute phase of stroke, and at which a prospective registry was maintained. Data from other centers were more scarce, oftentimes nonconsecutive, explaining our pragmatic decision so as to limit biases linked to patients in which perfusion was performed

The current analysis was restricted to patients with pre-treatment DSC perfusion sequence of adequate quality for post-processing. Due to the motion-sensitive nature of the post-processing method used in this work, slight to moderate diffusion/perfusion artifacts led to exclusion for the current work whereas only patients with marked artefact were excluded in the previous reported manuscript. In turn, 34 additional patients were deemed ineligible for the current analysis because of insufficient imaging quality compared to the previously reported analyses (See Flowchart in online-only figure I).

Imaging analysis

Post-processing and images' interpretation were performed centrally after complete de-identification, by an internal core-lab, blinded to clinical data. See Figure 1 for a detailed visual representation of imaging post-processing.

Ischemic lesion segmentation

Perfusion maps were generated using the Olea-Sphere® 3.0 software (olea-medical.com). Having verified all automated outputs and manually corrected artifacts, we performed the segmentation of both ischemic core lesions (Apparent Diffusion Coefficient (ADC) of 0.6×10^{-3} mm²/s or less) and critically hypo-perfused lesions (Tmax > 6 seconds)¹⁵ using a semi-automatic method with the Mango® software (MANGO, v3.1.1, Research imaging Institute, UTHSCSA), as described before.⁶

For the sake of clarity, the acronyms Diffusion Weighted Imaging (DWI) and Perfusion Weighted Imaging (PWI) have been used hereinafter to designate respectively core lesions and critically hypo-perfused lesions (that is, the core and the penumbral volume)

Atlas registration and labelling of the main brain regions

Diffusion-weighted and perfusion lesion masks were co-registered to the standard MNI-152 template using the FSL Software (<https://fsl.fmrib.ox.ac.uk/fsl/fslwiki>).¹⁶ We mapped the “JHU DTI based white-matter atlases” and “the Automated Anatomical Labelling (AAL)” atlases of brain white and grey matter regions respectively in the MNI-152 space referential, and computed the overlap of the segmented DWI and PWI lesions with each individual brain region, allowing to derive within each region the volume of infarcted and critically hypo-perfused brain tissue.

Definition of eloquent regions

Based on previous knowledge of brain regional relevance with regards to 3-month mRs derived from Voxel-based Lesion Symptom Mapping (VLSM) studies^{10–12,17,18},

we highlighted in the anatomic atlases, the brain regions with High Eloquent (HE). See Figure 2.

Definition of imaging variables

DWI and PWI volumes were labelled according to their overlap with HE brain regions. DWI volume of HE regions was defined as “high-eloquence infarct” (HE-I), and the PWI volume of HE regions was defined as “high-eloquence critically hypoperfused tissue (i.e.penumbra)” (HE-P). Using these intermediate variables, we explored eloquent mismatch ratios (E-MR) at two different levels:

- First, at the regional level, where the mismatch ratio (Region-E-MR) was defined as the ratio of PWI volume to the DWI volume within each individual region.

- Second, at the “eloquent group level” where regions in the same eloquence group were considered a whole. In this second analysis, we defined the High Eloquent Mismatch Ratio (HE-MR) as the sum of the Region-E-MR in the HE group divided by the number of regions in this group.

Global Mismatch Ratio (G-MR) was defined according to previous large studies, and as previously described,⁶ as the total PWI volume divided by the DWI volume.

Substantial reperfusion after MT was defined as a modified TICl score of 2b, 2b or 3.¹⁹

Study endpoints

The primary endpoint was a favourable functional outcome, defined as a modified Rankin scale (mRS) of 0-3, taking into account the inherent severity of AIS with baseline LIC, and in line with recent literature in this subgroup.²⁰ Sensitivity analyses analyzed the functional independence defined as mRS of 0-2.²¹

Statistical Analysis

Statistical analysis was performed using JMP Pro 14 (SAS Institute Inc. 2015. JMP® Pro 14. Cary, NC: SAS Institute Inc) software. Continuous variables were

summarized using means (\pm standard deviation, SD) or median [interquartile ranges, IQR] where appropriate, and discrete variables were summarized using counts (percentages).

We compared baseline characteristics of patients in the MT and control groups. Chi-square test, Fisher's exact test, t test, Mann-Whitney U test were used as appropriate for the univariable analysis, with a p-value < 0.05 (two-tailed) as the threshold for statistical significance. Multivariable analyses were adjusted for five prespecified baseline prognostic variables (age, diabetes mellitus, internal carotid artery (ICA) occlusion, intravenous fibrinolysis (i.v.tPA), delay between symptom-onset (or symptoms discovery if unwitnessed stroke) to imaging) as per previous knowledge on clinical imaging predictors of outcome after AIS-LVO.²²

We tested two distinct approaches to study the effect of incorporating the functional relevance of both infarcted and hypo-perfused brain tissue in determining functional outcome:

- First we compared the predictive accuracy for favourable functional outcome (mRS 0-3) of the "standard model" (that included only the global infarct volume [G-I] and the global mismatch ratio [G-MR] as imaging variables) with two other statistical models where only the involvement of the brain tissue with High Eloquence were considered. In the standard model (model 1), the G-I and the G-MR were entered into a binary logistic regression model amongst the other clinical outcome predictors. Model 2 was built similarly with HE-I and HE-MR instead of G-I and G-MR, hence exploring the functional relevance at the "eloquent group level". Model 3 relied on a bootstrap random forest approach, where the mismatch within each HE region was seen as an independent variable, alongside the HE-I and the clinical outcome predictors. In the two binary logistic regression models (model 1 and model 2), the

interaction between mismatch ratio (G-MR in model 1 and HE-MR in model 2, respectively) and MT was tested by including the multiplicative mismatch-ratio-by-treatment term in regression models. This approach was repeated with analogous models (models 1bis, 2bis and 3bis) using functional independence (mRS 0-2) as the dependent variable. To compare the predictive accuracy of the different models, we built contingency matrix and ROC curves (c-Statistic) and computed Precision, Accuracy and Balance Accuracy for randomly selected training sets (75% of the data) and testing sets (25% of the data).

- The second approach aimed to test whether a patients' selection based on the HE-MR could increase the treatment effect of MT as well as the subset of patients which might be identified as benefiting from this treatment, in comparison to a selection based on the G-MR. Hence, the number needed to treat (NNT, i.e. $1/\text{absolute risk reduction}$) to achieve mRS 0-3 with MT versus BMM was calculated for a range of G-MR and HE-MR thresholds.

RESULTS

Baseline characteristics of MT group versus BMM group

Between January 2015 and July 2018, 96 patients were included and analyzed in the MT group. Before 2015, a total of 154 patients with DWI-ASPECTs 0-6 were screened for inclusion in the BMM group, and 42 met study criteria. A total of 138 patients were hence analyzed (n=96 in the MT group and n=42 in the BMM group). A flowchart of patients' selection is presented in Online-only Figure I. Baseline characteristics are detailed in Table 1. Compared with the BMM group, patients in the MT group were younger ($67.3\pm 15y$ vs $77.6\pm 13.5y$; $p<0.001$), more frequently females (40.6% vs 19%; $p<0.014$), more frequently transferred patients (i.e. "drip&ship patients", 21.9% vs 0%; $p<0.001$) and received less frequently i.v.tPA (45.8% vs 100%; $p<0.001$). Demographics, past medical history and baseline clinical assessment were similar between patients treated with MT or BMM.

Mean G-I and G-P volumes were $100.4\text{ml}\pm 36.3\text{ml}$ and $157.6\pm 56.2\text{ml}$ respectively and did not differ between groups. Mean HE-I and HE-P were 70.7 ± 30.6 ml and 85.5 ± 37.8 ml respectively and did not differ between groups. At three months, 60/133 (45.1%) patients had a favourable functional outcome (mRS 0-3), with no difference amongst groups (49.5% in the MT group vs 39.7%; $p=0.14$). Altogether, 34/133 (25.6%) were functionally independent, with no difference amongst groups (26.4% in the MT group vs 23.8%; $p=0.138$). Symptomatic intracranial hemorrhage occurred in 29/129 (22.5%) patients and 41/133 (30.8%) patients were deceased at 3 months with no difference between groups (both $p>0,05$).

Models' accuracy for 3 months functional outcome

Primary endpoint: Favourable functional outcome (mRS 0-3)

In Model 1, independent predictors of 3-month favourable functional outcome included lower age (adjusted odd ratio, aOR 0.96 [0.93-0.98]; $p=0.01$), lower G-MR

(0.15 [0.04-0.52]; $p < 0.01$), lower G-I (aOR 0.98 [0.96-0.99]; $p < 0.01$), and medical history of diabetes mellitus. See online-only Table I. There was no significant interaction between MT effect and G-MR ($p = 0.17$).

In Model 2, independent predictors of 3-month favourable functional outcome included: receiving MT (aOR 7.74 [1.24-48.24]; $p = 0.016$), lower age (aOR 0.94 [0.90-0.97]; $p < 0.01$), lower HE-MR (aOR 0.02 [0.01-0.26]; $p < 0.01$), lower HE-I (aOR 0.96 [0.94-0.97]; $p < 0.01$) and medical history of diabetes mellitus. See online-only Table II. There was a significant interaction between MT effect and HE-MR $p = 0.045$.

In the bootstrap random forest model 3, the first ten variables identified as the strongest 3-month favourable functional outcome predictors were: receiving MT (adjusted effect, aEF = 1), the absence of ICA occlusion (aEF = 1), lower HE-I (aEF = 0.401), decreasing age (aEF = 0.381) and the presence of eloquent mismatch within the following regions: the right thalamus (aEF = 0.243), the left thalamus (aEF = 0.188), the left superior longitudinal fasciculus (aEF = 0.179), the left post central gyrus (aEF = 0.145), the left retrolenticular part of internal capsule (aEF = 0.140) and the left supra marginal gyrus (aEF = 0.137). See Online-only Table III and Online-only Figure III. Predictive performance of the three models are summarized in Table 2 and Online-only Figure II. Models considering the functional relevance of the infarct location showed a better predictive accuracy for favourable functional outcome with a c-Statistic of testing sets of 0.76 and 0.83 for logistic regression model 2 and bootstrap random forest model 3 respectively. In comparison, the logistic regression model 1, based on the global mismatch showed a c-Statistic of testing set 0.67. Nonetheless, model 3 showed a slight weakest consistency between training set and testing set with a decreasing c-Statistic from 1 to 0.83 (versus 0.82 to 0.67 and 0.88 to 0.76 for model 1 and 2, respectively) likely indicating overfitting of the training set.

In sensitivity analyses, using mRs 0-2 as the outcome measure, similarly to the primary outcome, bootstrap random forest (Model 3bis) was the most accurate to predict 3-month functional independence outcome compared to the two logistic regression models (model 1bis and model 2bis, please see the online-only Tables IV to VII, Online-only Appendix, and Figure IV).

Global mismatch ratio and Eloquent mismatch ratio and the number needed to treat (NNT)

To explore the effect of incorporating functional relevance of penumbral and infarcted regions in the selection process for MT of patients with AIS-LVO and a LIC, we explored the variation of the NNT, based on G-MR (that is, not considering the eloquence) or HE-MR (that is, by factoring the extent of persistent mismatch in high eloquence regions).

Decreasing G-MR threshold was associated with a rapidly increasing NNT and the treatment effect of MT was no longer significant above a G-MR threshold of 1.6. In turn the largest subset of patient identified as benefitting from MT when patients' selection relied on G-MR was 68/138 (48.57% of the cohort). Conversely, using decreasing HE-MR threshold, the NNT increased more gradually and the treatment effect of MT remained significant above a HE-MR threshold of 0.2 (see figure 3 and Online-only table VIII for aOR and NNT associated with thresholds). In turn if patients' selection relied on HE-MR, the largest subset of patient identified as benefitting from MT was 107/138 (76.43% of the cohort).

DISCUSSION

In this multicenter cohort of patient with AIS-LVO and LIC at baseline, we demonstrated that: 1) In models considering the functional relevance of the infarct location, the predictive accuracy of both favourable functional outcome and functional independence models at 3-months was strengthened; 2) In such models, the interaction between treatment effect of MT and mismatch was reinforced; 3) Using a functional relevance based mismatch, we reduced the risk of over selection by showing a better outcome in a larger subset of patients after MT and by demonstrating a compelling reduction of the NNT for comparable subgroup size.

These results derive from rather complex analyses but can be summarized in a very clinically pertinent and routinely applicable way: in patients with large infarct core at baseline, those with persisting salvageable tissue in high eloquent regions have higher odds of favourable functional recovery if treated with MT, and the treatment effect of MT in determining favourable functional outcome is much more important in this subgroup than in that with no eloquent area in salvageable regions. In turn, when considering a patient with a large infarct for MT, the analysis of the involvement of eloquent brain regions in the infarct core may help for decision making.

The influence of ischemic lesion location on stroke recovery is long known, and has been already reported in several studies^{11,23,24} However, in most studies such topographic parameters were usually considered only by assessing the infarct core (using MRI diffusion, CT-Perfusion or Noncontrast-CT), oftentimes after the hyperacute phase. Our results provide valuable additional arguments on the role of functional eloquence of lesion location, by allowing their analysis as a core/perfusion mismatch in the initial assessment of AIS patients. This approach was driven by the underlying hypothesis that the benefit of ischemic stroke treatment, aiming to

reestablish flow to hypo perfused but still viable (i.e. 'at-risk' or 'salvageable') brain tissue would be maximum in patients with salvageable tissue located in high eloquent brain regions, and paltry in contrast for patients with salvageable tissue located in poor eloquent regions.

The eloquent region map was defined a priori according to dedicated VLSM studies, which is amongst the most informative imaging-based statistical method to determine lesion location significance for stroke outcomes,^{10,11,23} and strongly correlates with anatomical-functional correlations. In our sample, the bootstrap random forest models highlighted several regions as having the most direct impact on stroke recovery. Both models, found a strong lateralization with more regions associated with poor outcome on the left hemisphere, in accordance with previous studies.^{11,23} Both thalamus and two left white matter fiber tracts (the superior longitudinal fasciculus and the cortico-spinal tract) were identified as strongly reducing the probability of favourable functional outcome, when involved (model 3). The strong impact of the thalamic injuries was unexpected since being rare in anterior circulation ischemic stroke. By contrast, posterior limbs of the internal capsules have not been identified as key structures in the bootstrap model, despite the fact that they convey the cortico-spinal tracts, which are long known to be amongst key functional regions, due to the dramatic motor impairment associated with its injury.^{25,26} Both results are very likely the consequences of a multifactorial lack of spatial resolution making difficult the distinction between small contiguous areas after co-registration. In turn considering the capsulo-thalamic region, rather than distinguishing thalamus and internal capsule, should be preferable in similarly built models. The superior longitudinal fasciculus is a thick white matter fiber tract linking the four lobes in each hemisphere. It plays a pivotal role in key processes

such as attention, memory, emotions and language and his implication in poor mRS when injured is in line with both VLSM^{10,23} and diffusion tensor imaging (DTI)^{27,28} studies.

Through the different models compared in this study, two different ways of considering the eloquent mismatch parameter have been explored. In logical regression models 2 and 2bis, the eloquent mismatch was seen as a whole. By contrast, in the bootstrap random forest models 3 and 3bis, the mismatch within each eloquent region was an independent variable. The later supervised learning approach yielded more accurate results in our sample to predict both favourable functional outcome and functional independence at 3-month, despite being slightly more sensitive to overfitting. However, we do acknowledge that such complex imaging-based patient's selection, especially when relying on machine learning algorithm with multiple variables, would not be realistic in current practice unless integrated in a dedicated software. Nonetheless, our analysis strengthens the argument that analyzing the infarct core independently of eloquent regions involvement likely results in over selection, that is to deny MT to patients that may have strongly benefitted by limiting infarct progression in hypo-perfused, yet not infarcted eloquent regions. The process of region identification, herein done with elaborated statistical tools, is moreover quite close to clinical practice, where the identification of eloquent regions involvement can be done visually at the time of patients' evaluation (i.e. "there's a large infarct in the anterior frontal areas, but the central and capsule-thalamic regions are not infarcted yes, despite being at-risk). In that sense, the individual region approach appears closer to bedside evaluation of per-region salvageability, than a global approach which doesn't seem reasonably doable in the clinical setting due to the multiple regions potentially involved or spared.

As previously discussed extensively in the literature,^{6,29} the matter of the precise selection of AIS-LVO patients likeliest to benefit from revascularization is subjected to important limits. Indeed, as the complexity of clinical imaging selection increases, the number of patients being denied treatment is likely to decrease. It is unlikely that abrupt thresholds (ASPECTs < 6, DWI > 70 or 100ml) have any pathophysiological rationale, and are in turn responsible for an important overselection (e.g. a patient with a 71ml right anterior frontal infarct, but a 150ml critically hypoperfused region involving the central region is likely deleterious). The underlying question is whether MT is harmful for some patients (large infarct cores, older individuals, ...), or if such an invasive and expensive treatment is appropriate when the odds of favourable functional outcome are very low. Altogether, our results only emphasize that LIC is not per se a good argument to deny MT, and that the consideration of eloquent regions may provide additional arguments in the face of genuine uncertainty.

Of note, there is ongoing debate on the concept of “ischemic core”,³⁰ for which the term severely ischemic tissue of uncertain viability (SIT-uv) may more accurately define the uncertainty of the tissue viability. The notion of “core” is indeed challenged, amongst other, by the fact that it cannot individually account for functional outcome, as is demonstrated in this work. For clarity we preferred the term “core” in this work so as not to overburden the manuscript with an additional acronym. Nonetheless, our results come as a confirmation that “core” volume alone cannot be used to anticipate functional outcome, and also emphasizes that simple (and thresholded) imaging variables should not be used to deny MT based on anticipated futility.

This study has limitations inherent to its retrospective design, including non-exhaustively risks of selection, memorization and attrition biases yielding a decrease in external applicability. We acknowledge that the BMM group was biased by the fact

that it included only patients who received i.v.tPA. This subselection may have yielded underestimated estimates of the benefit of MT over best medical management, in patients with persistent eloquent mismatch. Moreover, it is a selection bias that the MT data comes from eight different hospitals whereas the BMM group is from one center only. The use of MRI, first line imaging in almost all French Centers³¹ make our results less generalizable to geographic regions using CT

The strengths include a large sample size for this subgroup of patients, the use of advanced robust imaging post-processing methods, and the multicentric nature of data acquisition.

CONCLUSION

Integrating functional eloquence assessment of infarcted and critically hypoperfused brain regions on the baseline MRI of patients with AIS-LVO and LIC might improve the global framework of patients' selection for MT and can be easily transposed to clinical practice, by evaluating the involvement of high eloquence regions in the infarct core to evaluate the likelihood of MT benefit.

TABLES AND FIGURES

Table 1: Baseline Characteristics of included patients

| | MT (n=96) | BMM (=42) | Total (n=138) | p |
|-------------------------------------|------------------|------------------|------------------|--------|
| Patients characteristics | | | | |
| Age | 67.3±15.3 N=96 | 77.6±13.5 N=42 | 72.4±14.4 N=138 | <0.001 |
| Female sex | 40.6% (39/96) | 19% (8/42) | 34.1% (47/138) | 0.014 |
| Hypertension | 52.1% (50/96) | 57.1% (24/42) | 53.6% (74/138) | 0.583 |
| Diabetes Mellitus | 15.6% (15/96) | 14.3% (6/42) | 15.2% (21/138) | 0.841 |
| Dyslipidemia | 33.3% (32/96) | 47.6% (20/42) | 37.7% (52/138) | 0.111 |
| Tobacco use (current or past) | 29.2% (28/96) | 38.1% (16/42) | 31.9% (44/138) | 0.301 |
| Stroke Management | | | | |
| Baseline NIHSS score | 18.9±4.3 N=95 | 18.2±4.8 N=39 | 18.6±4.5 N=134 | 0.398 |
| Unwitnessed onset | 16.7% (16/96) | 16.7% (7/42) | 16.7% (23/138) | 1 |
| Drip & Ship | 21.9% (21/96) | 0% (0/42) | 15.2% (21/138) | <0.001 |
| Left-sided stroke | 55.2% (53/96) | 38.1% (16/42) | 50% (69/138) | 0.064 |
| Iv. tPA | 45.8% (44/96) | 100% (42/42) | 62.3% (86/138) | <0.001 |
| ICA occlusion | 18.8% (16/85) | 23.8% (10/42) | 20.5% (26/127) | 0.613 |
| M1 occlusion | 70.6% (60/85) | 61.9% (26/42) | 67.7% (86/127) | |
| Symptom-onset* to imaging | 152.3±103.5 N=86 | 157.7±107.6 N=42 | 155±105.5 N=128 | 0.788 |
| Symptom-onset* to needle | 159.5±44.4 N=38 | 189.5±90.3 N=38 | 174.5±67.4 N=76 | 0.071 |
| Symptom-onset* to groin | 303.9±104.4 N=71 | / | / | / |
| Imaging parameters | | | | |
| DWI ASPECTS | 4 [2-5] N=85 | 4 [3-5] N=40 | 4 [2-5] N=125 | 0.199 |
| Overall Core volume (in ml) | 101.6±39.2 N=96 | 99.1±33.3 N=42 | 100.4±36.3 N=138 | 0.709 |
| Overall Tmax<6s volume (in ml) | 165.8±60.5 N=96 | 149.4±52 N=42 | 157.6±56.2 N=138 | 0.129 |
| High Eloquence Core volume (in ml) | 67.8±31.9 N=96 | 77.6±26.3 N=42 | 70.7±30.6 N=138 | 0.062 |
| High Eloquence Tmax<6s (in ml) | 87.8±40.4 N=96 | 80.1±30.6 N=42 | 85.5±37.8 N=138 | 0.216 |
| Outcome measures | | | | |
| Successful reperfusion (mTICI 2b-3) | 83.7% (82/96) | / | / | / |
| 90 day mRS 0-2 | 26.4% (24/91) | 23.8% (10/42) | 25.6% (34/133) | 0.753 |
| 90 day mRS 0-3 | 49.5% (45/91) | 35.7% (15/42) | 45.1% (60/133) | 0.138 |
| 90 day Mortality | 29.7% (27/91) | 33.3% (14/42) | 30.8% (41/133) | 0.671 |
| sICH | 25.8% (24/93) | 13.9% (5/36) | 22.5% (29/129) | 0.146 |

Values are expressed as mean ± standard deviation (SD), or absolute value (percentage). Abbreviations: MT=Mechanical Thrombectomy; BMM= Best Medical Management; NIHSS=National Institutes of Health Stroke Scale; ASPECTs= Alberta Stroke Program Early CT Score; Iv. tPA= intravenous tissue plasminogen activator; ICA=Internal Carotid Artery; M1 and M2: first and second segment of the middle cerebral artery; mTICI= Modified Treatment in Cerebral Infarction Scale; sICH= Symptomatic Intracranial Haemorrhage; *Or symptoms discovery if unwitnessed stroke

Table 2: Predictive performance of the tree models for favourable functional outcome

| | Model 1 - Training | Model 1 - Testing | Model 2 - Training | Model 2 - Testing | Model 3 - Training | Model 3 - Testing |
|---------------------------|-------------------------------|------------------------------|-------------------------------|------------------------------|-------------------------------|------------------------------|
| Sensitivity | 75.00% | 73.33% | 75.61% | 71.43% | 100.00% | 68.75% |
| Specificity | 78.43% | 80.00% | 81.13% | 76.47% | 100.00% | 76.47% |
| Precision | 73.17% | 78.57% | 75.61% | 71.43% | 100.00% | 73.33% |
| Negative predictive value | 80.00% | 75.00% | 81.13% | 76.47% | 100.00% | 72.22% |
| Accuracy | 76.92% | 76.67% | 78.72% | 74.19% | 100.00% | 72.73% |
| Balance Accuracy | 76.72% | 76.67% | 78.37% | 73.95% | 100.00% | 72.61% |
| AUC-ROC | 0.82 [0.75-0.87] | 0.67 [0.56-0.86] | 0.88 [0.83-0.93] | 0.76 [0.69-0.94] | 1 | 0.83 |
| RMSE | 0.4157 | | 0.3923 | | 0.2393 | |
| AISc | 110.6 | | 101.88 | | / | |
| BIC | 133.02 | | 124.66 | | / | |

RMSE=Root Mean Squared Error; AISc=Corrected Akaike Information Criterion;
BIC=Bayesian Information Criterion

FIGURE LEGENDS

Figure 1: Algorithm Development Outline

G-I=Global diffusion volume; G-P= Global critically hypo-perfused tissue; HE-I=Diffusion volume in High eloquent regions; HE-P= High eloquent critically hypo-perfused tissue

Figure 2: Brain regions with high functional eloquence

Axial T1 weighted MRI template sections showing the 61 high functional eloquent brain regions.

Figure 3: NNT associated with Global mismatch ratio and Eloquent mismatch ratio thresholds

NNT=Number Needed to Treat; G-MR=Global Mismatch Ratio; HE-MR= Mismatch Ratio in High Eloquent Regions

REFERENCES

1. Román LS, Menon BK, Blasco J, et al. Imaging features and safety and efficacy of endovascular stroke treatment: a meta-analysis of individual patient-level data. *Lancet Neurol.* 2018;17:895–904.
2. Turc G, Bhogal P, Fischer U, et al. European Stroke Organisation (ESO) - European Society for Minimally Invasive Neurological Therapy (ESMINT) Guidelines on Mechanical Thrombectomy in Acute Ischemic Stroke. *J Neurointerventional Surg.* Epub 2019 Feb 26.
3. Powers WJ, Rabinstein AA, Ackerson T, et al. Guidelines for the Early Management of Patients With Acute Ischemic Stroke: 2019 Update to the 2018 Guidelines for the Early Management of Acute Ischemic Stroke: A Guideline for Healthcare Professionals From the American Heart Association/American Stroke Association. *Stroke.* 2019;50:e344–e418.
4. Cagnazzo F, Derraz I, Dargazanli C, et al. Mechanical thrombectomy in patients with acute ischemic stroke and ASPECTS ≤ 6 : a meta-analysis. *J Neurointerventional Surg.* 2020;12:350–355.
5. Shih LC, Saver JL, Alger JR, et al. Perfusion-weighted magnetic resonance imaging thresholds identifying core, irreversibly infarcted tissue. *Stroke.* 2003;34:1425–1430.
6. Kerleroux B, Janot K, Dargazanli C, et al. Perfusion Imaging to Select Patients with Large Ischemic Core for Mechanical Thrombectomy. *J Stroke.* 2020.
7. Nogueira RG, Jadhav AP, Haussen DC, et al. Thrombectomy 6 to 24 Hours after Stroke with a Mismatch between Deficit and Infarct. *N Engl J Med.* 2018;378:11–21.
8. Albers GW, Marks MP, Kemp S, et al. Thrombectomy for Stroke at 6 to 16 Hours with Selection by Perfusion Imaging. *N Engl J Med.* 2018;378:708–718.
9. Menezes NM, Ay H, Wang Zhu M, et al. The real estate factor: quantifying the impact of infarct location on stroke severity. *Stroke.* 2007;38:194–197.
10. Cheng B, Forkert ND, Zavaglia M, et al. Influence of stroke infarct location on functional outcome measured by the modified rankin scale. *Stroke.* 2014;45:1695–1702.
11. Munsch F, Sagnier S, Asselineau J, et al. Stroke Location Is an Independent Predictor of Cognitive Outcome. *Stroke.* 2016;47:66–73.
12. Wu O. Beyond Lesion Volumes: Network-based Approach for the Investigation of Neurocognitive Deficits in Patients with Chronic Subcortical Strokes. *Radiology.* 2018;288:195–197.
13. JENI Research Collaboration. A call for junior interventional neuroradiologists to join the JENI-Research Collaboration. *J Neuroradiol* 2018;45:341-342. Epub 2018 Jul 15.
14. von Elm E, Altman DG, Egger M, et al. The Strengthening the Reporting of Observational Studies in Epidemiology (STROBE) statement: guidelines for reporting observational studies. *Lancet Lond Engl.* 2007;370:1453–1457.
15. Lansberg MG, Straka M, Kemp S, et al. MRI profile and response to endovascular reperfusion after stroke (DEFUSE 2): a prospective cohort study. *Lancet Neurol.* 2012;11:860–867.

16. Fonov V, Evans A, McKinstry R, Almlí C, Collins D. Unbiased nonlinear average age-appropriate brain templates from birth to adulthood. *NeuroImage*. 2009;47:S102.
17. Phan TG, Demchuk A, Srikanth V, et al. Proof of concept study: relating infarct location to stroke disability in the NINDS rt-PA trial. *Cerebrovasc Dis Basel Switz*. 2013;35:560–565.
18. Timpone VM, Lev MH, Kamalian S, et al. Percentage insula ribbon infarction of >50% identifies patients likely to have poor clinical outcome despite small DWI infarct volume. *AJNR Am J Neuroradiol*. 2015;36:40–45.
19. Goyal M, Fargen KM, Turk AS, et al. 2C or not 2C: defining an improved revascularization grading scale and the need for standardization of angiography outcomes in stroke trials. *J NeuroInterventional Surg*. 2014;6:83–86.
20. Kaesmacher Johannes, Chaloulos-Iakovidis Panagiotis, Panos Leonidas, et al. Mechanical Thrombectomy in Ischemic Stroke Patients With Alberta Stroke Program Early Computed Tomography Score 0–5. *Stroke*. 2019;50:880–888.
21. Fiorelli M, Bastianello S, Kummer R von, et al. Hemorrhagic Transformation Within 36 Hours of a Cerebral Infarct Relationships With Early Clinical Deterioration and 3-Month Outcome in the European Cooperative Acute Stroke Study I (ECASS I) Cohort. *Stroke*. 1999;30:2280–2284.
22. Campbell BCV, Majoie CBLM, Albers GW, et al. Penumbra imaging and functional outcome in patients with anterior circulation ischaemic stroke treated with endovascular thrombectomy versus medical therapy: a meta-analysis of individual patient-level data. *Lancet Neurol*. 2019;18:46–55.
23. Wu O, Cloonan L, Mocking SJT, et al. Role of Acute Lesion Topography in Initial Ischemic Stroke Severity and Long-Term Functional Outcomes. *Stroke*. 2015;46:2438–2444.
24. Ernst M, Boers AMM, Aigner A, et al. Association of Computed Tomography Ischemic Lesion Location With Functional Outcome in Acute Large Vessel Occlusion Ischemic Stroke. *Stroke*. 2017;48:2426–2433.
25. Lindenberg R, Renga V, Zhu LL, Betzler F, Alsop D, Schlaug G. Structural integrity of corticospinal motor fibers predicts motor impairment in chronic stroke. *Neurology*. 2010;74:280–287.
26. Zhu LL, Lindenberg R, Alexander MP, Schlaug G. Lesion load of the corticospinal tract predicts motor impairment in chronic stroke. *Stroke*. 2010;41:910–915.
27. Kamali A, Flanders AE, Brody J, Hunter JV, Hasan KM. Tracing Superior Longitudinal Fasciculus Connectivity in the Human Brain using High Resolution Diffusion Tensor Tractography. *Brain Struct Funct* [online serial]. 2014;219. Accessed at: <https://www.ncbi.nlm.nih.gov/pmc/articles/PMC3633629/>. Accessed April 27, 2020.
28. Breier JI, Hasan KM, Zhang W, Men D, Papanicolaou AC. Language dysfunction after stroke and damage to white matter tracts evaluated using diffusion tensor imaging. *AJNR Am J Neuroradiol*. 2008;29:483–487.
29. Nogueira Raul G., Ribó Marc. Endovascular Treatment of Acute Stroke. *Stroke*. American Heart Association; 2019;50:2612–2618.

30. Goyal Mayank, Ospel Johanna M., Menon Bijoy, et al. Challenging the Ischemic Core Concept in Acute Ischemic Stroke Imaging. *Stroke*. American Heart Association; 2020;51:3147–3155.
31. Forestier G, Kerleroux B, Janot K, et al. Mechanical thrombectomy practices in France: exhaustive survey of centers and individual operators. *J Neuroradiol J Neuroradiol*. Epub 2020 May 13.

APPENDIX 1: AUTHORS CONTRIBUTIONS

| Name | Affiliation | Role | Contribution |
|-----------------------------|-------------------------------------|--------|--|
| Basile KERLEROUX, MD | Sainte-Anne Hospital, Paris, France | Author | Design and conceptualized study; analyzed the data; drafted the manuscript for intellectual content; Major role in the acquisition of data; Performed biostatistical review of results |
| Joseph BENZAKOUN, MD | Sainte-Anne Hospital, Paris, France | Author | Design and conceptualized study; analyzed the data; drafted the manuscript for intellectual content; Major role in the acquisition of data |
| Kevin JANOT, MD | CHRU Tours, France | Author | Major role in the acquisition of data; Revisions for critical intellectual content |
| Cyril DARGAZANLI, MD | Montpellier Hospital, France | Author | Major role in the acquisition of data; revised the manuscript for intellectual content |
| Dimitri DALY ERAYA, MD | Montpellier Hospital, France | Author | Major role in the acquisition of data |
| Wagih BEN HASSEN, MD | Sainte-Anne Hospital, Paris, France | Author | Major role in the acquisition of data; revised the manuscript for intellectual content |
| François ZHU, MD | CHU Nancy, France | Author | Major role in the acquisition of data; revised the manuscript for intellectual content |
| Benjamin GORY, MD-PhD | CHU Nancy, France | Author | Major role in the acquisition of data; revised the manuscript for intellectual content |
| Jean François HAK, MD | CHU Timone, Marseille France | Author | Major role in the acquisition of data |
| Charline PEROT, MD | CHU Timone, Marseille France | Author | Major role in the acquisition of data; revised the manuscript for intellectual content |
| Lili DETRAZ, MD | CHU Nantes, France | Author | Major role in the acquisition of data; revised the manuscript for intellectual content |
| Romain BOURCIER, MD-PHD | CHU Nantes, France | Author | Major role in the acquisition of data; revised the manuscript for intellectual content |
| Aymeric ROUCHAUD, MD-PhD | CHU Limoges, France | Author | Major role in the acquisition of data; revised the manuscript for intellectual content |
| Géraud FORESTIER, MD | CHU Limoges, France | Author | Major role in the acquisition of data; revised the manuscript for intellectual content |
| Gaultier MARNAT, MD | CHU Bordeaux, France | Author | Major role in the acquisition of data; revised the manuscript for intellectual content |
| Florent GARIEL, MD | CHU Bordeaux, France | Author | Major role in the acquisition of data; revised the manuscript for intellectual content |
| Pasquale MORDASINI, MD | CH Bern, Switzerland | Author | Revised the manuscript for intellectual content |
| Pierre SENERS, MD-PhD | Fondation Rothschild, Paris, France | Author | Revised the manuscript for intellectual content |
| Guillaume TURC, MD-PhD | Sainte-Anne Hospital, Paris, France | Author | Revised the manuscript for intellectual content |
| Johannes KAESMACHER, MD | CH Bern, Switzerland | Author | Major role in the acquisition of data; revised the manuscript for intellectual content |
| Catherine OPPENHEIM, MD-PhD | Sainte-Anne Hospital, Paris, France | Author | Revised the manuscript for intellectual content; supervision |
| Olivier NAGGARA, MD-PhD | CHRU Lille, France | Author | Major role in the acquisition of data; revised the manuscript for intellectual content; supervision |
| Grégoire BOULOUIS, MD | Sainte-Anne Hospital, Paris, France | Author | Design and conceptualized study; analyzed the data; drafted the manuscript for intellectual content; Major role in the acquisition of data |

SUPPLEMENTAL MATERIAL

Relevance of Brain Regions' Eloquence Assessment in Patients with Large Ischemic Cores treated with Mechanical Thrombectomy.

Basile KERLEROUX^{1,2*} MD, Joseph BENZAKOUN MD,^{1*} Kevin JANOT² MD-MSc, Cyril DARGAZANLI³ MD-MSc, Dimitri DALY ERAYA³ MD, Wagih BEN HASSEN¹ MD-MSc, François ZHU⁴ MD-MSc, Benjamin GORY⁴ MD-PhD, Jean François HAK⁵ MD-MSc, Charline PEROT⁶ MD, Lili DETRAZ⁷ MD-MSc, Romain BOURCIER⁷ MD-PhD, Aymeric ROUCHAUD⁸ MD-PhD, Géraud FORESTIER⁸ MD, Gaultier MARNAT⁹ MD, Florent GARIEL⁹ MD, Pasquale MORDASINI¹⁰ MD, Pierre SENER¹¹ MD-PhD, Guillaume TURC¹² MD-PhD, Johannes KAESMACHER¹⁰ MD, Catherine OPPENHEIM¹ MD-PhD, Olivier NAGGARA¹ MD-PhD, Grégoire BOULOUIS^{1,2} MD-MSc-FESO On behalf of the JENI Research Collaborative.

*Equal contribution as first authors

¹ INSERM U1266, Institut of Psychiatry and Neuroscience (IPNP), UMR_S1266, INSERM, Université de Paris, GHU Paris Psychiatrie et Neurosciences, site Sainte-Anne, Neuroradiology Department, Université de Paris, des Neurosciences Psychiatrie de Paris

² Diagnostic and Therapeutic Neuroradiology, CHRU de Tours, 2 bd Tonnelé, Tours France

³ Department of Interventional Neuroradiology, University Hospital Center of Montpellier, Gui de Chauliac hospital, Montpellier, France

⁴ Université de Lorraine, CHRU-Nancy, Department of Diagnostic and Therapeutic Neuroradiology, F-54000 Nancy, France and Université de Lorraine, IADI, INSERM U1254, F-54000 Nancy, France

⁵ Department of Diagnostic and Interventional Neuroradiology, Timone Hospital, Aix Marseille University, APHM, Cedex, France

⁶ Neurology Department, Timone Hospital, Aix Marseille University, APHM, Cedex, France.

⁷ Department of Diagnostic and Interventional Neuroradiology, Guillaume et René Laennec University Hospital, Nantes, France

⁸ Department of interventional neuroradiology, Dupuytren University Hospital, 2 Avenue Martin Luther King, 87000 Limoges, France.

⁹ Department of Diagnostic and Interventional Neuroradiology, Pellegrin Hospital - University Hospital of Bordeaux, Place Amélie Raba-Léon, 33076 Bordeaux, France.

¹⁰ Institute of Diagnostic, Interventional and Pediatric Radiology and Institute of Diagnostic and Interventional Neuroradiology, University Hospital Bern, Inselspital, University of Bern, Bern, Switzerland

¹¹ Neurology Department, Fondation Rothschild Hospital, Paris, France

¹² Neurology Department, GHU Paris Psychiatrie et Neurosciences, Université de Paris, INSERM U1266, FHU NeuroVasc, Paris, France

Correspondance: B. Kerleroux, Neuroradiology-department, GHU-Paris, 1 rue Cabanis, 75014 Paris. basile.kerleroux@gmail.com Tel: +33145658574 Fax: +33145658574

This online only material contains :

One supplemental Appendix, 8 supplemental Tables and 4 Supplemental Figures.

Supplemental Appendix: Sensitivity analysis with mRs 0-2 as endpoint

In Model 1bis, lower G-I (0.78 [0.66-0.94]; $p < 0.01$) was the only variable independently associated with 3-month functional independence. There was no significant interaction between MT effect and G-MR $p = 0.72$. See Supplemental Table IV for details.

In Model 2bis, independent predictors of 3-month functional independence were lower age (aOR 0.94 [0.92-0.99]; $p < 0.01$); lower HME-I (aOR 0.95 [0.93-0.97]; $p < 0.01$), lower HME-MR (aOR 0.01 [0.00-0.33] and receiving iv.tPA (aOR 3.61 [1.03-12.68]; $p = 0.04$). There was a significant interaction between MT effect and HME-MR $p = 0.03$. See Supplemental Table V for details.

In the bootstrap random forest model 3bis, the first ten variables identified as the strongest determinants of 3-month functional independence were, receiving MT treatment (adjusted effect, aEF = 1), no ICA occlusions (aEF = 1), decreasing age (aEF = 0.403), lower HME-I (aEF = 0.343), lower symptom-onset to imaging (aEF = 0.187) and the presence of eloquent mismatch within the following areas: the left temporal superior gyrus (aEF = 0.243), the left superior longitudinal fasciculus (aEF = 0.231), the left supra marginal gyrus (aEF = 0.224), the left insula (aEF = 0.201), the left external capsule (aEF = 0.201) and the left middle temporal gyrus (aEF = 0.183). See Supplemental Table VI and Supplemental Figure IV. Predictive performance of the tree models are summarized in Supplemental Table 7. Similarly, to the primary outcome, bootstrap random forest Model 3bis was the most accurate to predict 3-month functional independence outcome compared to the two logistic regression models (model 1bis and model 2bis).

Supplemental Tables

Supplemental Table I: Logistic regression model 1 for favourable functional outcome

| Variables | Odds ratio [IC 95%] | p |
|-----------------------------------|----------------------------|------------------|
| Age (In years) | 0.96 [0.93-0.98] | 0.013 |
| Diabetes Mellitus | 0.11 [0.02-0.75] | 0.014 |
| ICA occlusion (vs MCA) | 0.33 [0.08-1.36] | 0.112 |
| G-I (per ml increase) | 0.98 [0.96-0.99] | >0.001 |
| G-MR (per unit increase) | 0.15 [0.04-0.52] | 0.002 |
| Symptom-onset* to imaging | 1 [1-1] | 0.994 |
| Iv. tPA | 3.09 [0.85-11.19] | 0.098 |
| Received MT | 3.47 [0.86-14.07] | 0.073 |
| Interaction G-MR* Treatment group | / | 0.168 |

ICA=Internal Carotid Artery; MCA= Middle Cerebral Artery; G-I=Global diffusion volume; G-MR= Global Mismatch Ratio; Iv. tPA= intravenous tissue plasminogen activator; MT= Mechanical Thrombectomy *Or symptoms discovery if unwitnessed stroke

Supplemental Table II: Logistic regression model 2 for favourable functional outcome

| Variables | Odds ratio [IC 95%] | p |
|-------------------------------------|----------------------------|------------------|
| Age (In years) | 0.94 [0.90-0.97] | <0.001 |
| Diabetes Mellitus | 0.1 [0.01-0.87] | 0.024 |
| ICA occlusion (vs MCA) | 0.5 [0.11-2.24] | 0.363 |
| Symptom-onset* to imaging | 1 [0.99-1] | 0.909 |
| HE-I (per ml increase) | 0.96 [0.94-0.97] | <0.001 |
| HE-MR (per unit increase) | 0.02 [0.01-0.26] | 0.001 |
| Iv.tPA | 3.51 [0.86-14.28] | 0.072 |
| Received MT | 7.74 [1.24-48.24] | 0.016 |
| Interaction HE-MR* traitement group | / | 0.044 |

ICA=Internal Carotid Artery; HE-I=Diffusion volume in high eloquent areas; HE-MR= Mismatch Ratio in high eloquent areas; Iv. tPA= intravenous tissue plasminogen activator; MT= Mechanical Thrombectomy *Or symptoms discovery if unwitnessed stroke

Supplemental Table III: Bootstrap random forest 3 for favourable functional outcome

| Variable | Adjusted Effect |
|--|------------------------|
| Received MT | 1 |
| No ICA occlusion | 1 |
| HE-I | 0.401 |
| Age | 0.381 |
| Hcprm 77 Thalamus_R 7101 | 0.243 |
| Hcprm 78 Thalamus_L 7102 | 0.188 |
| Hcprm 242 Superior_longitudinal_fasciculus_L | 0.179 |
| Hcprm 58 Postcentral_L 6002 | 0.145 |
| Hcprm 222 Retrolenticular_part_of_internal_capsule_L | 0.14 |
| Hcprm 64 SupraMarginal_L 6212 | 0.137 |
| Hcprm 37 Hippocampus_R 4101 | 0.133 |
| Symptom-onset* to imaging | 0.116 |
| Hcprm 12 Frontal_Inf_Oper_L 2302 | 0.104 |
| Hcprm 82 Temporal_Sup_L 8112 | 0.103 |
| Hcprm 228 Posterior_corona_radiata_L | 0.101 |
| Hcprm 30 Insula_L 3002 | 0.1 |
| Hcprm 203 Genu_of_corpus_callosum | 0.094 |
| Hcprm 234 External_capsule_L | 0.085 |
| Hcprm 227 Posterior_corona_radiata_R | 0.083 |
| Hcprm 65 Angular_R 6221 | 0.082 |
| Hcprm 86 Temporal_Mid_L 8202 | 0.08 |
| Hcprm 225 Superior_corona_radiata_R | 0.08 |
| Hcprm 221 Retrolenticular_part_of_internal_capsule_R | 0.063 |
| Hcprm 226 Superior_corona_radiata_L | 0.063 |
| Hcprm 246 Uncinate_fasciculus_L | 0.057 |
| iv. tPA | 0.05 |
| Hcprm 29 Insula_R 3001 | 0.046 |
| Hcprm 204 Body_of_corpus_callosum | 0.043 |
| Hcprm 219 Posterior_limb_of_internal_capsule_R | 0.041 |
| Diabetes Mellitus | 0.035 |
| Hcprm 220 Posterior_limb_of_internal_capsule_L | 0.034 |
| Hcprm 38 Hippocampus_L 4102 | 0.021 |

MT= Mechanical Thrombectomy; ICA=Internal Carotid Artery; HE-I=Diffusion volume in high eloquent areas; iv. tPA= intravenous tissue plasminogen activator; *Or symptoms discovery if unwitnessed stroke

Supplemental Table IV: Logistic regression model 1bis for functional independence

| Variables | Odds ratio [IC 95%] | p |
|---------------------------|----------------------------|------------------|
| Age (In years) | 0.97 [0.94-1.00] | 0.234 |
| Diabetes Mellitus | 0.64 [0.1-4.14] | 0.63 |
| ICA occlusion (vs MCA) | 0.57 [0.12-2.76] | 0.479 |
| G-I (per ml increase) | 0.78 [0.66-0.94] | <0.001 |
| G-MR (per ml increase) | 0.07 [0.01-3.56] | 0.093 |
| Symptom-onset* to imaging | 1 [1-1] | 0.991 |
| iv. tPA | 3.44 [0.83-14.21] | 0.077 |
| Received MT | 2.33 [0.59-9.17] | 0.217 |
| Interaction Mismatch*G-MR | / | 0.724 |

ICA=Internal Carotid Artery; G-I=Global diffusion volume; G-MR= Global Mismatch Ratio; Iv. tPA= intravenous tissue plasminogen activator; MT= Mechanical Thrombectomy *Or symptoms discovery if unwitnessed stroke

Supplemental Table V: Logistic regression model 2bis for functional independence

| Variables | Odds ratio [IC 95%] | p |
|-----------------------------|----------------------------|------------------|
| Age (In years) | 0.94 [0.92-0.99] | 0.007 |
| Diabetes Mellitus | 0.68 [0.1-4.41] | 0.679 |
| ICA occlusion (vs MCA ?) | 0.72 [0.15-3.5] | 0.678 |
| HE-I (per ml increase) | 0.95 [0.93-0.97] | <0.001 |
| HE-MR (per unit increase) | 0.01 [0.00-0.33] | 0.018 |
| Symptom-onset* to imaging | 1 [1-1.01] | 0.704 |
| iv. tPA | 3.61 [1.03-12.68] | 0.04 |
| Received MT | 4.09 [0.52-32.37] | 0.150 |
| Interaction Mismatch* HE-MR | / | 0.032 |

ICA=Internal Carotid Artery; HE-I=Diffusion volume in high eloquent areas; HE-MR= Mismatch Ratio in in high eloquent areas; Iv. tPA= intravenous tissue plasminogen activator; MT= Mechanical Thrombectomy *Or symptoms discovery if unwitnessed stroke

Supplemental Table VI: Bootstrap random forest 3bis for functional independence

| Variables | Adjusted Effect |
|--|------------------------|
| Reiceived MT | 1 |
| No ICA occlusion | 1 |
| Age | 0.403 |
| HE-I | 0.343 |
| Hcprm 82 Temporal_Sup_L 8112 | 0.243 |
| Hcprm 242 Superior_longitudinal_fasciculus_L | 0.231 |
| Hcprm 64 SupraMarginal_L 6212 | 0.224 |
| Hcprm 30 Insula_L 3002 | 0.201 |
| Hcprm 234 External_capsule_L | 0.201 |
| Symptom-onset* to imaging | 0.187 |
| Hcprm 86 Temporal_Mid_L 8202 | 0.183 |
| Hcprm 228 Posterior_corona_radiata_L | 0.181 |
| Hcprm 222 Retrolenticular_part_of_internal_capsule_L | 0.179 |
| Hcprm 58 Postcentral_L 6002 | 0.165 |
| Hcprm 204 Body_of_corpus_callosum | 0.141 |
| Hcprm 246 Uncinate_fasciculus_L | 0.134 |
| Hcprm 12 Frontal_Inf_Oper_L 2302 | 0.127 |
| Hcprm 226 Superior_corona_radiata_L | 0.12 |
| Hcprm 38 Hippocampus_L 4102 | 0.104 |
| Hcprm 37 Hippocampus_R 4101 | 0.095 |
| Hcprm 65 Angular_R 6221 | 0.091 |
| Hcprm 78 Thalamus_L 7102 | 0.09 |
| Hcprm 227 Posterior_corona_radiata_R | 0.084 |
| Hcprm 29 Insula_R 3001 | 0.082 |
| Hcprm 77 Thalamus_R 7101 | 0.076 |
| Hcprm 220 Posterior_limb_of_internal_capsule_L | 0.06 |
| Hcprm 203 Genu_of_corpus_callosum | 0.056 |
| Hcprm 221 Retrolenticular_part_of_internal_capsule_R | 0.054 |
| Hcprm 219 Posterior_limb_of_internal_capsule_R | 0.053 |
| Hcprm 225 Superior_corona_radiata_R | 0.052 |
| Diabetes Mellitus | 0.021 |
| iv. tPA | 0.014 |

MT= Mechanical Thrombectomy; ICA=Internal Carotid Artery; HE-I=Diffusion volume in high eloquent areas; iv. tPA= intraveinuous tissue plasminogen activator; *Or symptoms discovery if unwitnessed stroke

Supplemental Table VII: Predictive performance of the tree models for functional independence

| | Model 1 - Training | Model 1 - Testing | Model 2 - Training | Model 2 - Testing | Model 3 - Training | Model 3 - Testing |
|---------------------------|-------------------------------|------------------------------|-------------------------------|------------------------------|-------------------------------|------------------------------|
| Sensitivity | 50.00% | 20.00% | 60.00% | 50.00% | 100.00% | 50.00% |
| Specificity | 79.75% | 72.00% | 83.54% | 77.78% | 100.00% | 81.48% |
| Precision | 27.27% | 12.50% | 40.91% | 25.00% | 100.00% | 37.50% |
| Negative predictive value | 91.30% | 81.82% | 91.67% | 91.30% | 100.00% | 88.00% |
| Accuracy | 75.82% | 63.33% | 79.79% | 74.19% | 100.00% | 75.76% |
| Balance Accuracy | 64.87% | 46.00% | 71.77% | 63.89% | 100.00% | 65.74% |
| Error Rate | 24.18% | 36.67% | 20.21% | 25.81% | 0.00% | 24.24% |
| AUC-ROC | 0.8 [0.69-0.82] | 0.63 [0.48-0.84] | 0.84 [0.77-0.88] | 0.83 [0.78-0.99] | 1 | 0.8 |
| RMSE | 0.4027 | | 0.3601 | | 0.2285 | |
| AICc | 104.143 | | 97.7609 | | / | |
| BIC | 126.501 | | 120.543 | | / | |

RMSE=Root Mean Squared Error; AICc=Corrected Akaike Information Criterion; BIC=Bayesian Information Criterion

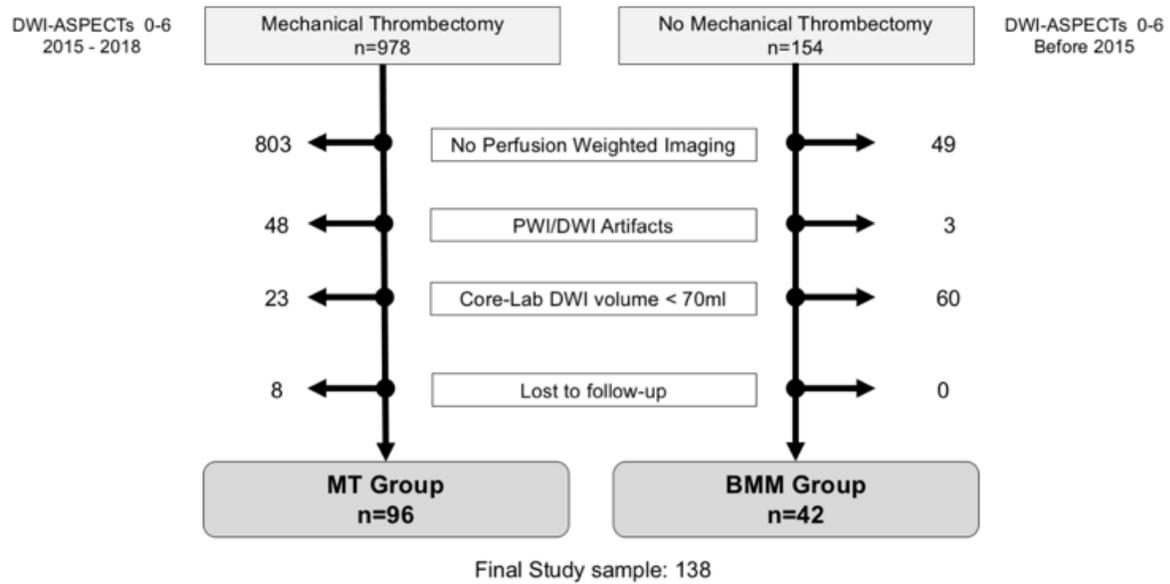
Supplemental Table VIII: aOR and NNT associated with Global mismatch ratio and**Eloquent mismatch ratio thresholds**

| G-MR Threshold | N | % of cohort | aOR* | p | BMM % mRS >3 | MT % mRS >3 | NNT |
|------------------------|----------|--------------------|-------------------|--------------|------------------------|-----------------------|------------|
| >1.7 | 48 | 34.29 | 7.75 [1.16-51.61] | 0.034 | 80 | 59 | 4.76 |
| >1.65 | 56 | 40.00 | 7.84 [1.39-44.11] | 0.019 | 78 | 54 | 4.17 |
| >1.6 | 63 | 45.00 | 5.13 [1.01-25.99] | 0.048 | 79 | 56 | 4.35 |
| >1.5 | 68 | 48.57 | 3.38 [0.74-15.42] | 0.116 | 76 | 56 | 5.00 |
| >1.4 | 76 | 54.29 | 2.64 [0.69-10.03] | 0.155 | 74 | 57 | 5.88 |
| >1.3 | 81 | 57.86 | 2.04 [0.61-6.9] | 0.249 | 69 | 57 | 8.33 |
| >1.2 | 92 | 65.71 | 2.03 [0.62-6.67] | 0.242 | 69 | 55 | 7.14 |
| >1.1 | 99 | 70.71 | 1.77 [0.56-5.62] | 0.333 | 68 | 56 | 8.33 |
| >1.05 | 103 | 73.57 | 1.59 [0.51-4.97] | 0.425 | 64 | 55 | 11.11 |
| HE-MR Threshold | N | % of cohort | aOR* | p | BMM % mRS >3 | MT % mRS >3 | NNT |
| >0.55 | 48 | 34.29 | 10.4 [1.19-90.82] | 0.034 | 82 | 52 | 3.33 |
| >0.48 | 54 | 38.57 | 9.47 [1.27-70.68] | 0.028 | 83 | 51 | 3.13 |
| >0.46 | 60 | 42.86 | 5.78 [1.01-33.15] | 0.049 | 80 | 52 | 3.57 |
| >0.45 | 64 | 45.71 | 3.86 [1.18-19.04] | 0.037 | 75 | 52 | 4.35 |
| >0.4 | 73 | 52.14 | 3.48 [1.22-14.73] | 0.041 | 74 | 53 | 4.76 |
| >0.35 | 83 | 59.29 | 4.77 [1.24-18.37] | 0.023 | 75 | 52 | 4.35 |
| >0.3 | 92 | 65.71 | 4.96 [1.4-17.65] | 0.01 | 76 | 48 | 3.57 |
| >0.2 | 107 | 76.43 | 3.6 [1.13-11.53] | 0.031 | 70 | 49 | 4.76 |
| >0.1 | 116 | 82.86 | 2.65 [0.89-7.92] | 0.081 | 68 | 50 | 5.56 |

G-MR= Global Mismatch Ratio; HE-MR= Mismatch Ratio in high eloquent areas; Iv. BMM= Best medical management; MT= Mechanical Thrombectomy

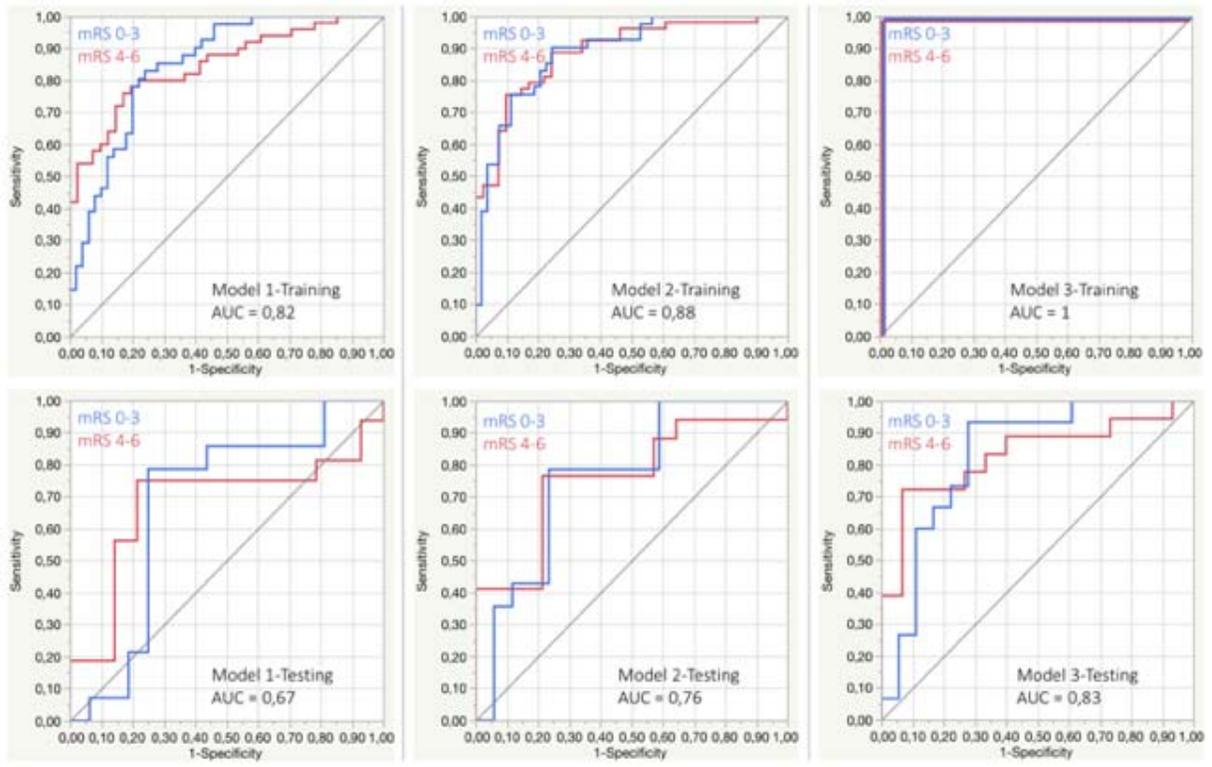
Supplemental Figures

Supplemental Figure I: Flowchart of patients' inclusions

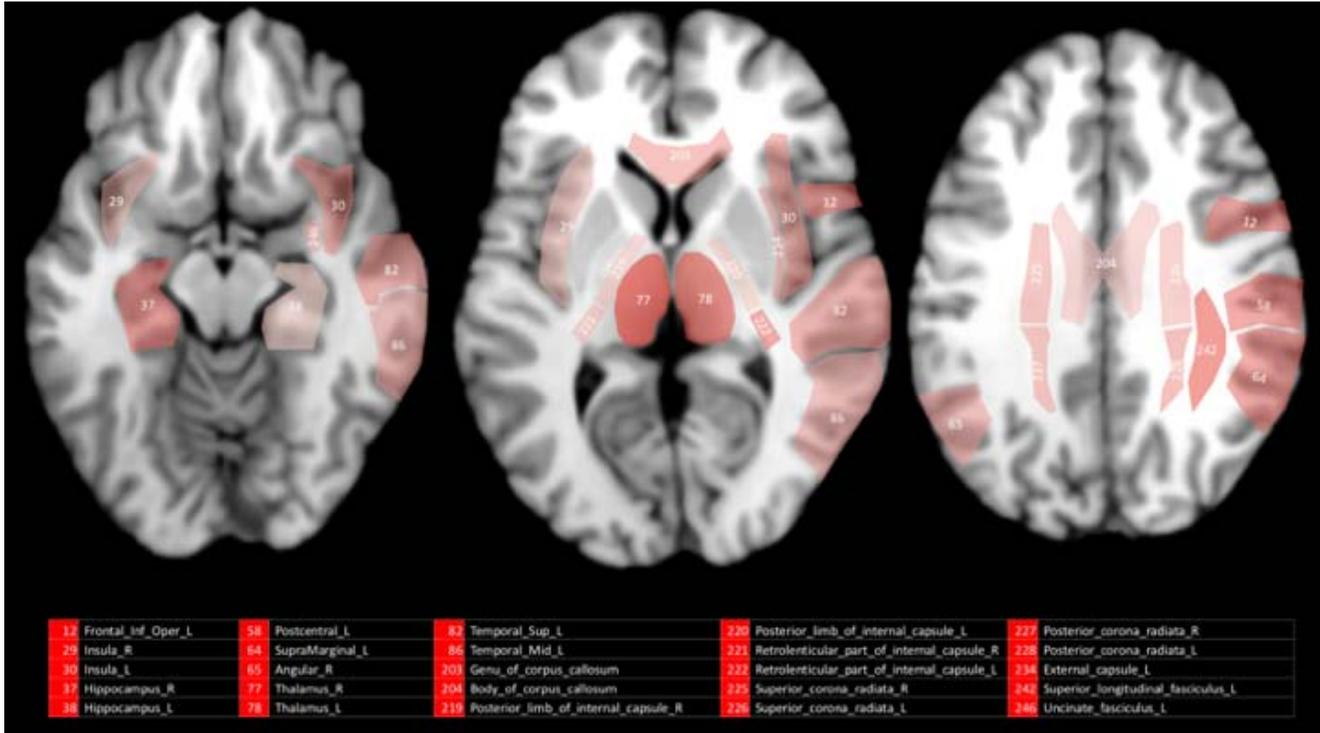


Abbreviations: MT=Mechanical Thrombectomy; BMM= Best Medical Management; PWI= Perfusion Weighted Imaging; DWI= Diffusion Weighted Imaging

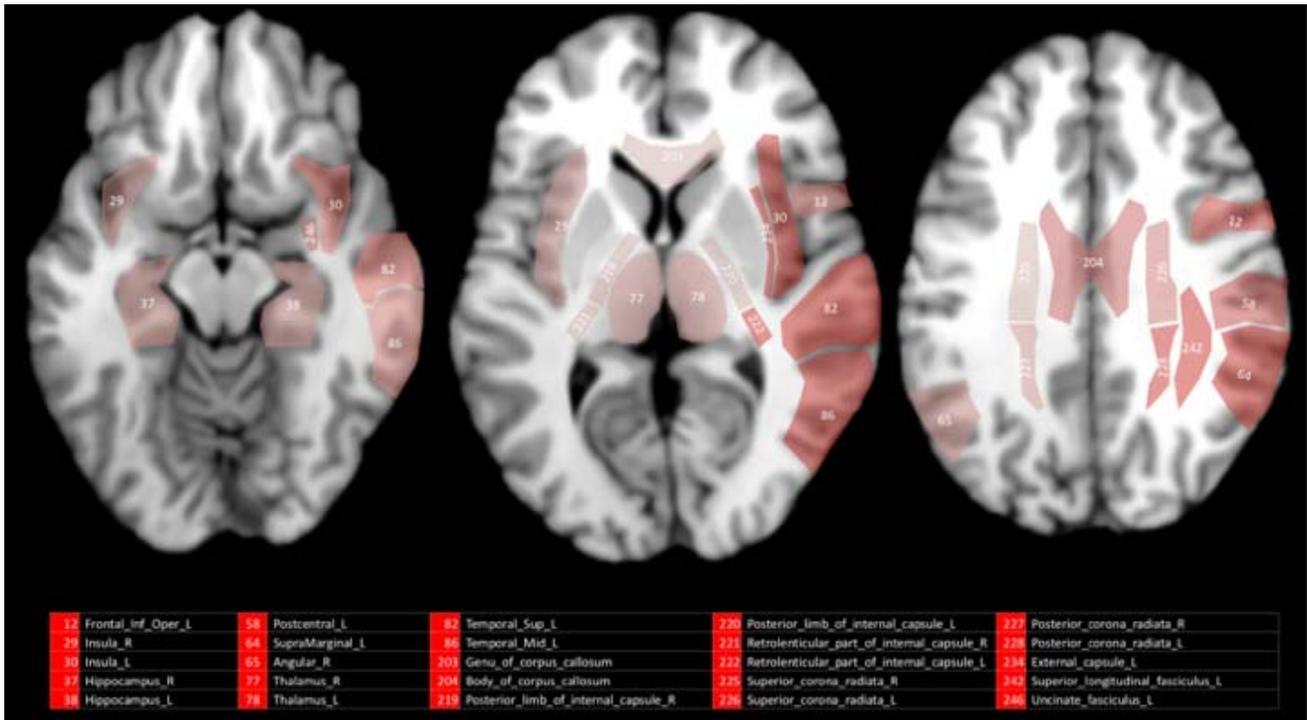
Supplemental Figure II: ROC curve of the tree models for favourable functional outcome

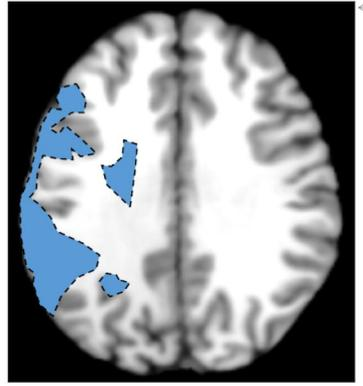
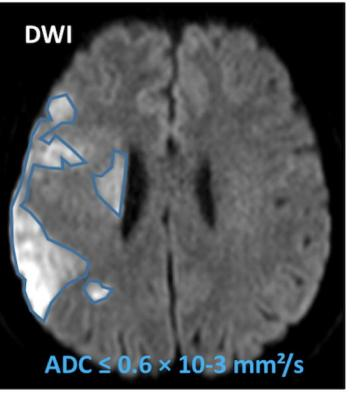


Supplemental Figure III: High eloquent areas ranking according to the bootstrap random forest model 3 for favourable functional outcome

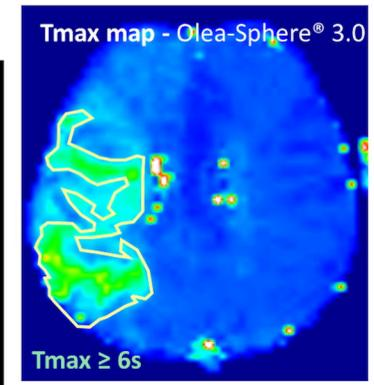
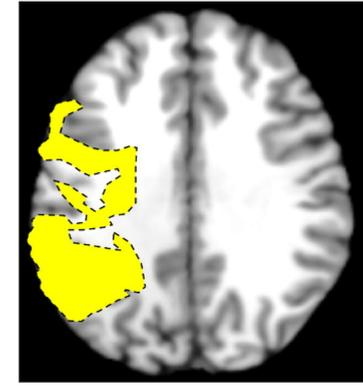
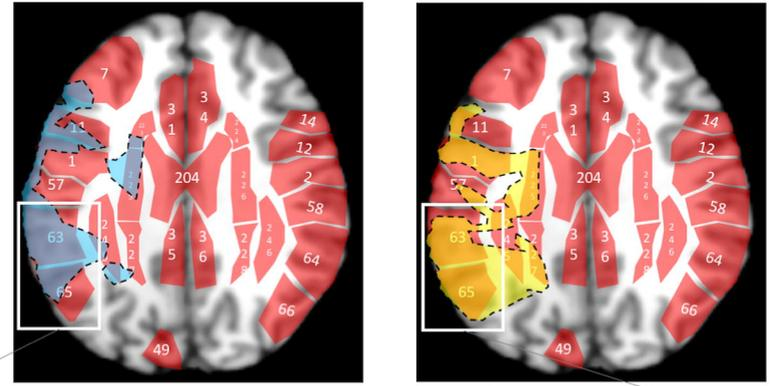


Supplemental Figure IV: High eloquent areas ranking according to the bootstrap random forest model 3bis for functional independence.

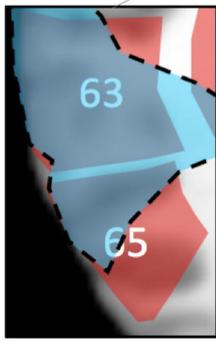




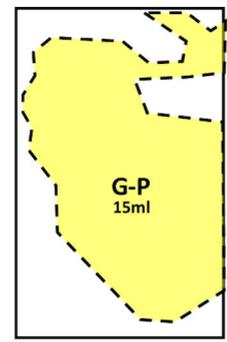
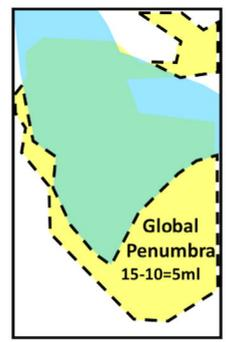
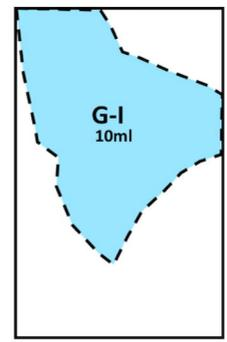
Ischemic lesion segmentation
MNI-152 template Registration
Mapping with Eloquent Atlases & Calculation of the overlap between the segmented DWI /PWI lesions and each eloquent region



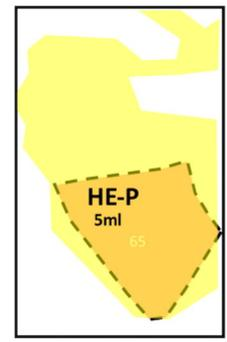
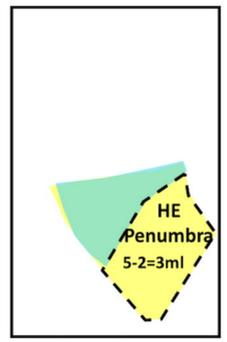
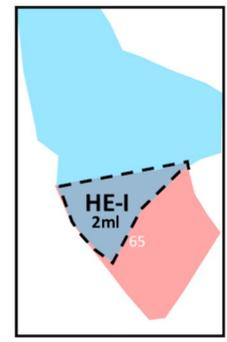
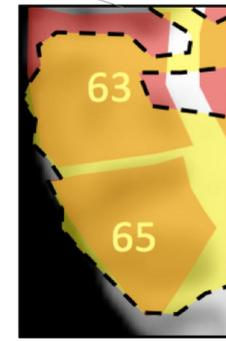
Global Mismatch Ratio = $G-P/G-I = 15/10 = 1,5$



Global approach
Eloquent approach

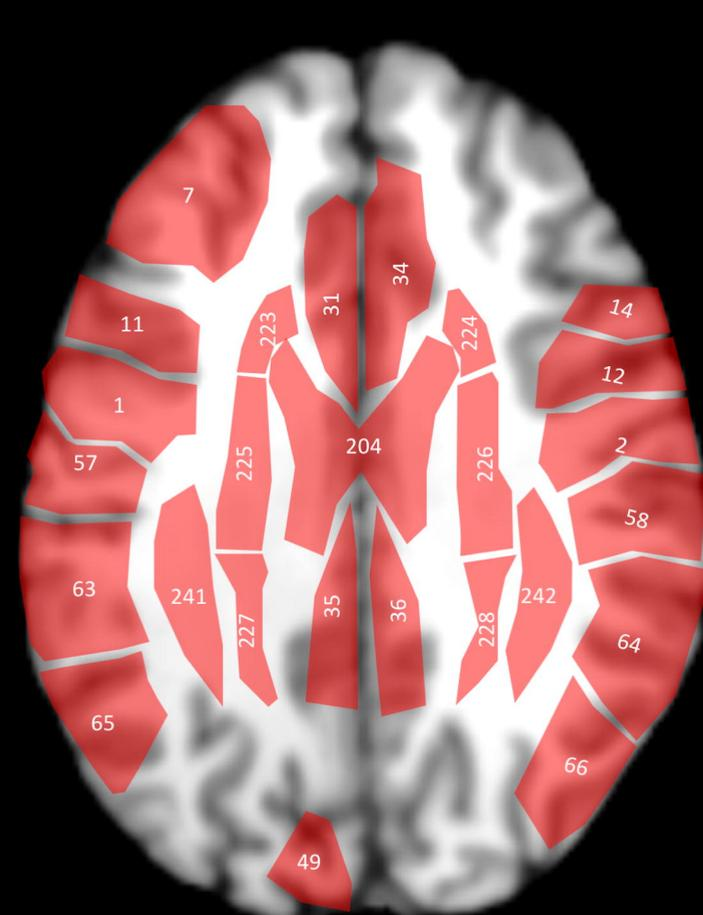
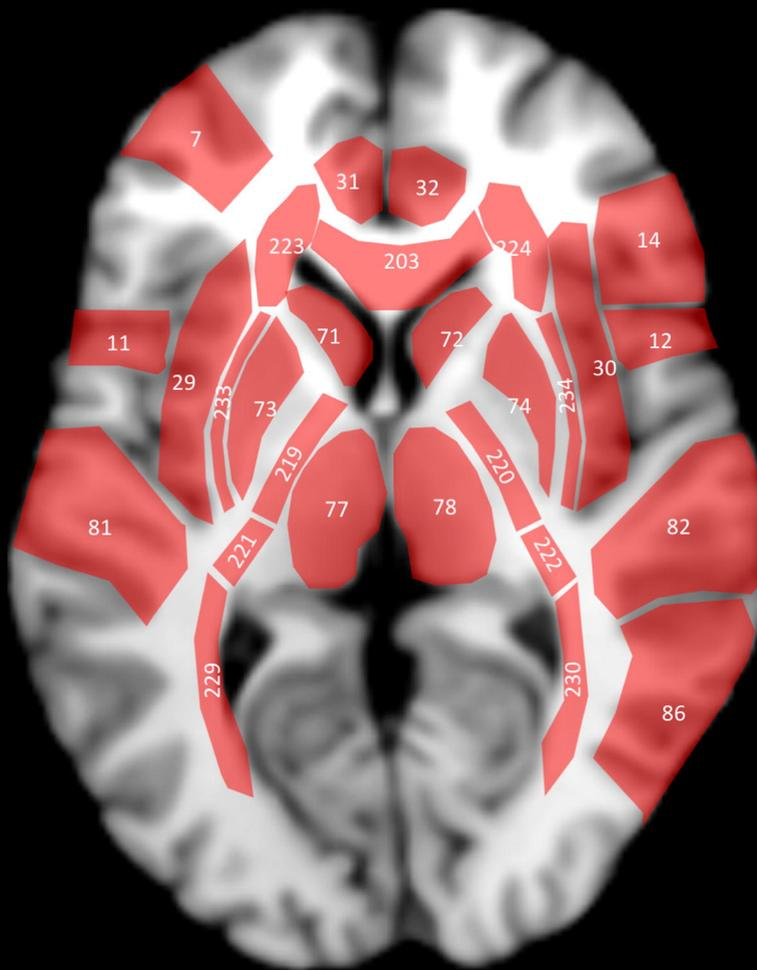
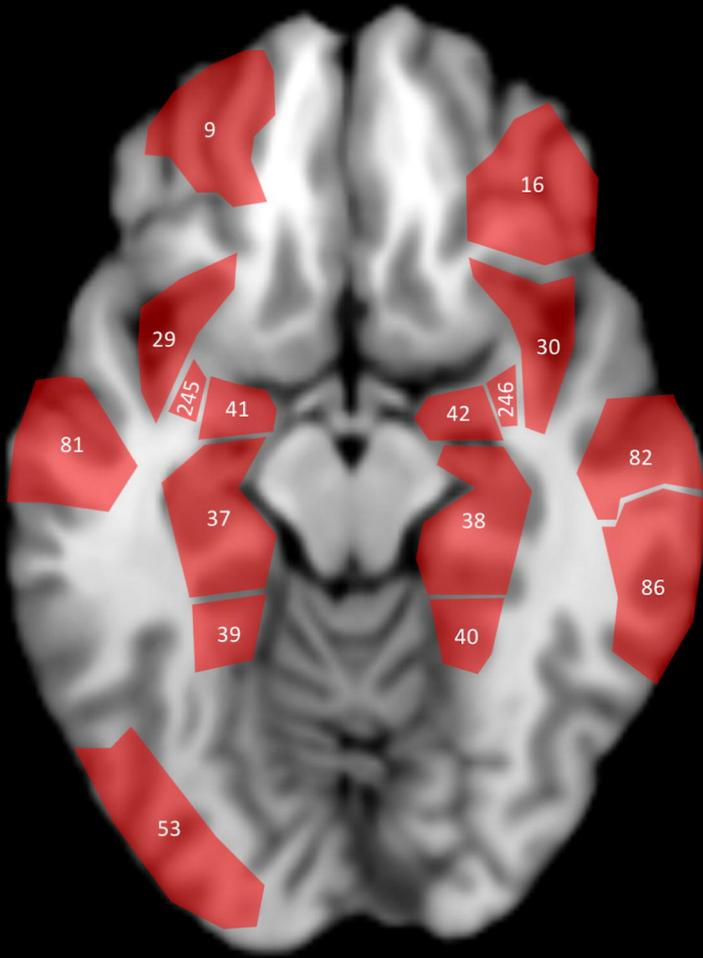


Global approach



Eloquent approach

High Eloquent Mismatch Ratio = $HE-P/HE-I = 5/2 = 2,5$



| | | | | | | | | | |
|----|--------------------|----|-------------------|-----|------------------------------------|-----|-------------------------|-----|--|
| 1 | Precentral_R | 36 | Cingulum_Post_L | 73 | Putamen_R | 12 | Frontal_Inf_Oper_L | 204 | Body_of_corpus_callosum |
| 2 | Precentral_L | 39 | ParaHippocampal_R | 74 | Putamen_L | 29 | Insula_R | 219 | Posterior_limb_of_internal_capsule_R |
| 7 | Frontal_Mid_R | 40 | ParaHippocampal_L | 81 | Temporal_Sup_R | 30 | Insula_L | 220 | Posterior_limb_of_internal_capsule_L |
| 9 | Frontal_Mid_Orb_R | 41 | Amygdala_R | 223 | Anterior_corona_radiata_R | 37 | Hippocampus_R | 221 | Retrolenticular_part_of_internal_capsule_R |
| 11 | Frontal_Inf_Oper_R | 42 | Amygdala_L | 224 | Anterior_corona_radiata_L | 38 | Hippocampus_L | 222 | Retrolenticular_part_of_internal_capsule_L |
| 14 | Frontal_Inf_Tri_L | 49 | Occipital_Sup_R | 229 | Posterior_thalamic_radiation_R | 58 | Postcentral_L | 225 | Superior_corona_radiata_R |
| 16 | Frontal_Inf_Orb_L | 53 | Occipital_Inf_R | 230 | Posterior_thalamic_radiation_L | 64 | SupraMarginal_L | 226 | Superior_corona_radiata_L |
| 28 | Rectus_L | 57 | Postcentral_R | 233 | External_capsule_R | 65 | Angular_R | 227 | Posterior_corona_radiata_R |
| 31 | Cingulum_Ant_R | 59 | Parietal_Sup_R | 241 | Superior_longitudinal_fasciculus_R | 77 | Thalamus_R | 228 | Posterior_corona_radiata_L |
| 32 | Cingulum_Ant_L | 63 | SupraMarginal_R | 245 | Uncinate_fasciculus_R | 78 | Thalamus_L | 234 | External_capsule_L |
| 33 | Cingulum_Mid_R | 66 | Angular_L | | | 82 | Temporal_Sup_L | 242 | Superior_longitudinal_fasciculus_L |
| 34 | Cingulum_Mid_L | 71 | Caudate_R | | | 86 | Temporal_Mid_L | 246 | Uncinate_fasciculus_L |
| 35 | Cingulum_Post_R | 72 | Caudate_L | | | 203 | Genu_of_corpus_callosum | | |

NNT

